Photo-CIDNP studies on reaction centers of rhodobacter sphaeroides

Prakash, Shipra

1 Introduction

1.1 Photosynthesis

1.1.1 Photosynthesis in bacteria and plants

Photosynthesis is the process by which solar energy is converted to chemical energy (Blankenship, 2002). Plants, algae and cyanobacteria perform oxygenic photosynthesis. In these organisms, light energy is used for reductive fixation of carbon dioxide into carbohydrates while oxidizing water. The produced carbohydrates serve as an energy source for both the photosynthetic organism itself and the non-photosynthetic organisms that directly or indirectly consume photosynthetic organisms. In addition to oxygenic photosynthesis, some organisms perform anoxygenic photosynthesis. These organisms are not capable of oxidizing water and instead they oxidize small inorganic or organic molecules such as hydrogen, hydrogen sulfide or organic acids to gain the reductive power. Anoxygenic photosynthetic bacteria can be classified into four groups of bacteria: the proteobacteria (purple bacteria), the green sulfur bacteria, the green filamentous bacteria and the heliobacteria (Imhoff, 1995; Madigan and Ormerod, 1995; Pierson and Castenholz, 1995; van Gemerden and Mas, 1995).

The primary processes of photosynthetic energy conversion are performed by pigment-protein complexes known as reaction centers (RCs). In general, two types of RCs have been characterized by the nature of their electron acceptors (Blankenship, 1992). The Type I RCs contain iron-sulfur clusters as their acceptors. The Type II RCs have a bacteriopheophytin and quinones as their electron acceptors. Purple bacteria and green filamentous bacteria have Type II RCs while the green sulfur bacteria and the heliobacteria contain Type I RCs. Both types of RCs are present in plants, algae and cyanobacteria. Photosystem I contains an iron-sulfur cluster and Photosystem II is of the pheophytin quinone type.

The purple bacteria may be further divided into two groups: purple sulfur bacteria and purple nonsulfur bacteria. Purple sulfur bacteria can grow in the presence of relatively high concentrations of reduced sulfur compounds like H_2S, while the same levels are toxic for purple nonsulfur bacteria (Brune, 1995). The work described in this thesis relates to the study of the electron-transfer process in RCs of the purple nonsulfur bacterium *Rhodobacter (Rb.) sphaeroides*.

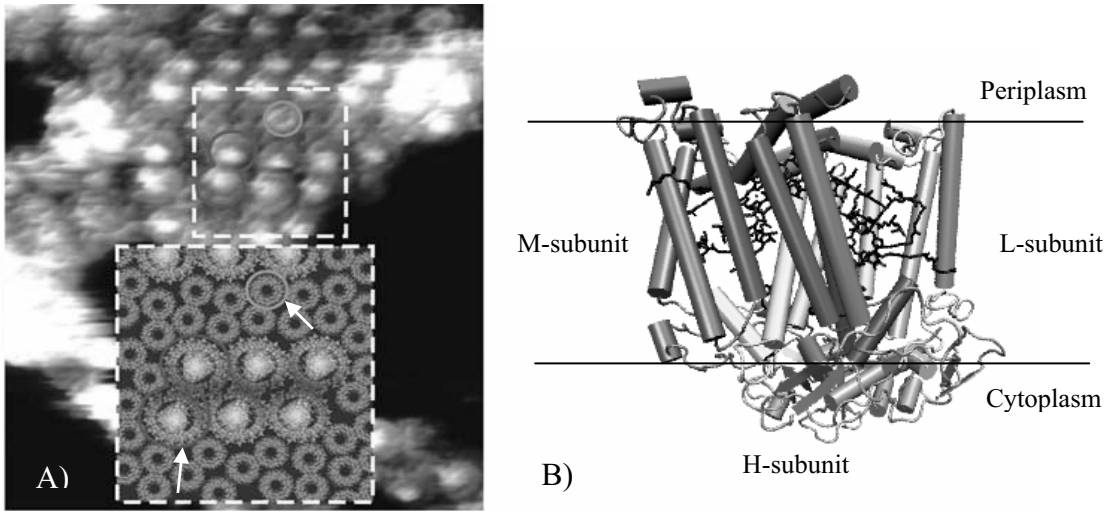

Figure 1.1. A) AFM picture of the PSU from *Rb. sphaeroides* WT consisting of the LH I-RC complex and the LH II surrounding it (shown by white arrows). The RC is present at the center of the LH I (Bahatyrova et al., 2004). B) Schematic representation of the RC in the membrane.

1.1.2 The Reaction Center of Rhodobacter sphaeroides

In the purple bacterium *Rb. sphaeroides*, the photosynthetic apparatus is located in vesicles inside the cytoplasmic membrane. Under anaerobic conditions, the cytoplasmic membrane invaginates and extends inward in vesicles forming the intracytoplasmic membranes. These can extend over the entire cytoplasm. In aerobic conditions of growth, the pigment synthesis and expression of the structural proteins involved in photosynthetic energy conversion is completely suppressed.

The photosynthetic apparatus of *Rb. sphaeroides* is a nanometric assembly in the intracytoplasmic membranes and consists mainly of two types of pigment-protein complexes, the RC and light harvesting (LH) complexes, LH I and LH II (Figure 1.1A). This complex of photosynthetic RC protein and the associated LHs is named the photosynthetic unit (PSU). The function of LHs is to capture sunlight and transfer the excitation energy to the RC. The LH I or B875, with a major absorption peak near 875 nm, surrounds the RC, while LH II, which is not in direct contact to the RC, absorbs maximally at 800 and 850 nm (Sündstrom and van Grondelle, 1995) (for review, see (Hu et al., 2002)).

The RC of *Rb. sphaeroides* is a transmembrane protein complex made of three major polypeptides, H, L and M (for heavy, medium and light) (Yeates et al., 1988; Ermler et al., 1994; Camara-Artigas et al., 2002) (Figure 1.1B). The L and M subunits contain five trans-membrane α-helices, which are packed together in a nearly symmetrical way. Subunit H is more globular in shape and is located mainly in the cytoplasmic side of the membrane. The L and M subunits bind the cofactors. Four molecules of bacteriochlorophyll *a* (BChl *a*), two molecules of bacteriopheophytin a (BPhe *a*), two ubiquinone-10 molecules (Q), a non-haem

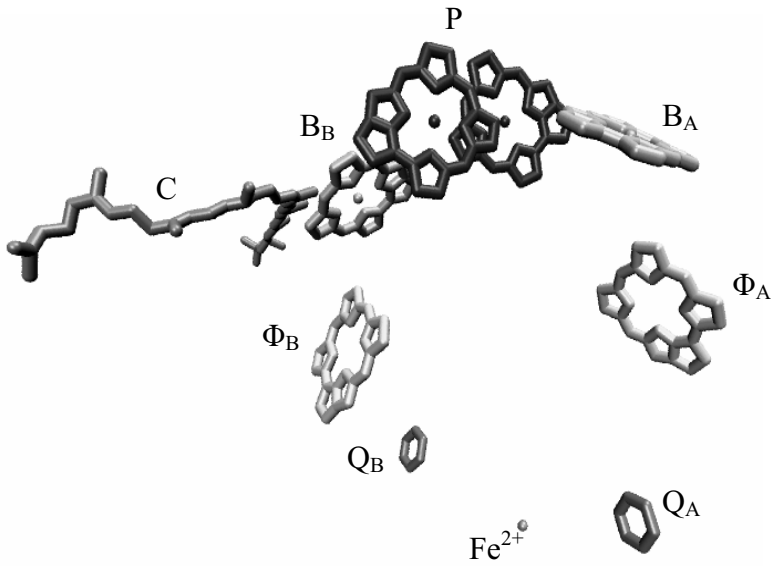

Figure 1.2. Cofactors of the RC of *Rb. sphaeroides WT*. The special pair (P) is a dimer of two BChl molecules. The accessory BChls (B), the bacteriopheophytins (Φ) and the ubiquinones (Q) are arranged in nearly a two fold symmetry. The carotenoid (C) is located in the inactive B-branch. The aliphatic chains from BChl, BPhe and Q are omitted for clarity.

iron (Fe^{2+}) and a caroteniod molecule (C) form the cofactors of the RC protein. The arrangement of the cofactors is shown in Figure 1.2. They are arranged in two nearly symmetric branches, the 'active' A-branch and the 'inactive' B-branch. Two BChls form a tightly interacting dimer called the 'Special Pair' (P). On either side of the special pair an additional BChl molecule is located, known as the accessory BChl (B_A and B_B). The two BPhe (Φ) are positioned 18 Å away from the special pair. Situated under the BPhe are the ubiquinones-10, (Q_A and Q_B). Finally, the non-haem Fe^{2+} ion is located in the center of the two branches near the cytoplasmic side of the membrane. The tenth cofactor, the carotenoid molecule (C), breaks the overall symmetry of the cofactor arrangement and is located near B_B. In the RC of *Rb. sphaeroides* R26, a mutant strain, no carotenoid molecule is present.

Despite symmetry in the structure, the electron-transfer pathway in the RC is asymmetric (for review, see Hoff and Deisenhofer, 1997). The electron transfer proceeds almost exclusively via the A branch. The reason for this functional asymmetry still remains unknown.

After photochemical excitation of P to P*, one electron is emitted which is transferred to the primary electron acceptor Φ_A within 3 ps, forming the radical pair state $P^{+\bullet}\Phi_A^{-\bullet}$(Martin et al., 1986). The $\Phi_A^{-\bullet}$ anion radical decays in about 200 ps and transfers an electron to the ubiquinone Q_A. The electron subsequently moves from Q_A to Q_B in 600 ms reducing Q_B once. Meanwhile, the oxidized primary electron donor P is re-reduced by accepting an electron from cytochrome c at the periplasmic side of the protein. The RC can be excited again and Q_A can give a second electron to Q_B. The doubly reduced and protonated Q_B leaves the RC to the

ubiquinone pool. New ubiquinone from the ubiquinone pool of the membrane replaces the ubiquinol leading to the intial state of the RC.

1.1.3 The Special Pair

The primary electron donor molecule (P) is a dimer formed of two strongly coupled BChl a molecules P_L and P_M corresponding to the polypeptide chains to which they are attached. P_L and P_M overlap in ring I of the BChl ring with an intermolecular distance of approximately 3.5 Å. The Mg atoms of both BChls are coordinated by a histidine ligand (His M202 and His L173).

It has been proposed that the excited state P^* is electronically asymmetric with more electron density on P_M as compared to P_L and this electronic asymmetry is related to the hydrogen-bonding environment of the keto groups (Moore et al., 1999). The electronic structure of the cation radical P^+ has been extensively investigated with EPR, ENDOR and TRIPLE resonance studies (Lendzian et al., 1993; Rautter et al., 1994; Lubitz et al., 2002). The studies have shown that the unpaired electron is unequally distributed over P_L and P_M favoring P_L with a ratio of 2:1. The observed asymmetry was attributed to the difference in energies of the highest filled molecular π-orbitals of the monomeric halves P_L and P_M, caused by differences in structure of the two BChls and/or the environment around the special pair (Lendzian et al., 1993). The knowledge of the electronic structure of P in the ground state is limited. Resonance Raman studies suggest that P_L and P_M are different in the ground state but no details are known (Mattioli et al., 1991; Palaniappan et al., 1993). The application of photochemically induced dynamic nuclear polarization (photo-CIDNP) MAS NMR in combination with site-directed ^{13}C-labeled BChl/BPheo RCs gave a first insight into the ground state electronic structure of the special pair at the atomic scale (Schulten et al., 2002). The studies showed that the ground state electronic structure of P is asymmetric due to the clearly distinct chemical shift patterns. This is interpreted in terms of different electron densities on both cofactors, presumably with higher electron density on P_L.

Current research has focused on applying photo-CIDNP MAS NMR towards building up the complete electronic ground state map of the special pair using site-directed ^{13}C-labeled BChl/BPheo RCs. Although the structure of the bacterial RC is known down to 2-3 Å resolution and the kinetics of the electron transfer has been determined, it is not yet clear how the special pair is tuned in the ground state to facilitate the emission of an electron. An essential parameter in electron transfer is the reorganization energy, which reflects the nuclear configuration associated with the charge transfer process. The involvement of the protein matrix in the emission of an electron from P is not yet clear. The reason for the functional asymmetry in the RC even though it has a very symmetric spatial structure is not known. In addition, the highly asymmetric ground state electronic structure of P with pronounced asymmetry on P_L requires further investigations. Finally, it is not clear whether the protein-

protein interactions inside the bacterial cell affect the local spin densities around the special pair, for example the interactions of LHCs with RCs. Such large systems with atomic resolution are not easily accessible with other spectroscopic methods. Photo-CIDNP MAS NMR even allows the study of RCs in intact cells.

1.2 Solid-State NMR

1.2.1 MAS NMR

NMR spectroscopy is an important tool for chemical analysis, structure determination and the study of dynamics in organic, inorganic and biological systems. Nowadays, it is used for a wide variety of applications from characterization of pharmaceutical products to determining structures of large molecules like polymers and proteins.

Although solution NMR is more routinely performed, solid-state magic-angle spinning (MAS) NMR is rapidly emerging as a powerful method for solid samples and materials. Solution NMR techniques are limited to smaller proteins (<100 kDa) and nucleic acids molecules. Solid-State NMR enables studies of large protein systems like membrane proteins, protein aggregates like prions, amyloids and nucleic acids that cannot be crystallized or are too large for solution NMR. In addition, it is possible with solid-state NMR to examine the functionally important internal dynamics in proteins and nucleic acids in absence of overall motion (Griffin, 1998; Laws et al., 2002). Magic-angle spinning (MAS) overcomes line-broadening by chemical shift anisotropy (CSA) in solids and allows detailed analysis of structure, dynamics and functional mechanisms of membrane-bound protein systems (de Groot, 2000; Zech et al., 2005). The principal limitation of NMR in general is its low sensitivity due to an unfavorable Boltzmann distribution caused by the small Zeeman splitting of nuclear spin levels. Nuclear magnetic moments are small ($\mu \approx 10^{-26}$ J/T), NMR frequencies are low (typically 10-500MHz) and nuclear spin polarizations at thermal equilibrium are small (typically $<10^{-5}$ at 300K). As a result, samples usually require in excess of 10^{17} NMR active nuclei to achieve acceptable signal-to-noise ratio. In general, for this reason NMR samples require isotope enrichment for less abundant nuclei like ^{13}C and ^{15}N. In solid-state NMR, the NMR lines are even broader, particularly in the case of homonuclear dipolar couplings which cannot be averaged completely with MAS.

1.2.2 Photo-CIDNP MAS NMR

Photochemically induced dynamic nuclear polarization (photo-CIDNP) provides a unique opportunity to probe the electronic structure of the special pair in the ground state at the atomic scale. Photo-CIDNP MAS NMR increases NMR intensities by induction of photochemical reactions, which shuffle the nuclear spin system out of its Boltzmann equilibrium. Photo-CIDNP chemical shift information refers to the electronic structure of the

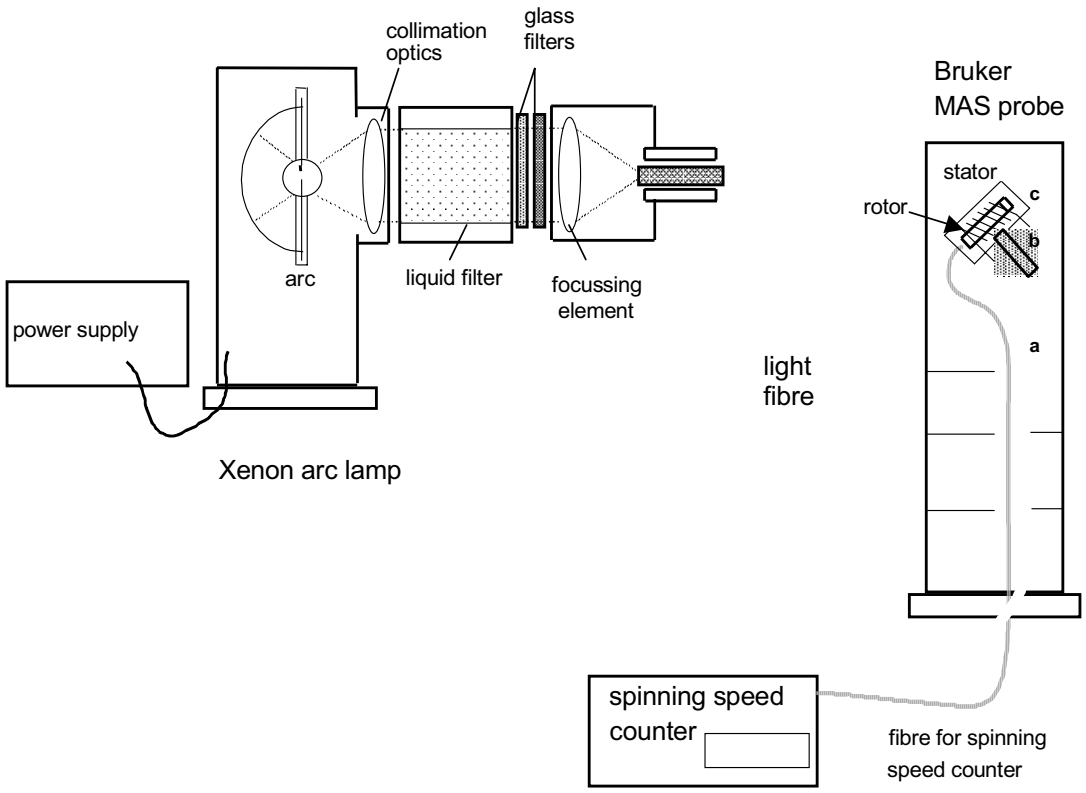

Figure 1.3. Schematic representation of the continuous illumination setup for a photo-CIDNP MAS NMR experiment (a,b,c refer to the points where the modification was made in the probe).

diamagnetic ground state after the photo-reaction and recombination and the intensities relate to the electron spin density distribution in $P^{+\bullet}\Phi_A^{-\bullet}$.

Photo-CIDNP was observed for the first time by solution NMR in 1967 (Bargon et al., 1967; Ward and Lawler, 1967). In the solid-state under continuous illumination, photo-CIDNP was observed for the first time in quinone-blocked frozen bacterial reaction centers (RCs) of *Rb. sphaeroides* R26 and WT (Zysmilich and McDermott, 1994, 1996b, 1996a; Matysik et al., 2000b; Matysik et al., 2001a; Schulten et al., 2002). Later studies on photosystem I of spinach led to a first set of assignments of the aromatic ring carbons to the P2 cofactor of the primary electron donor P700 (Alia et al., 2004b). In the D1D2 complex of the RC of the photosystem II of plants, the observation of a pronounced electron density on rings III and V by photo-CIDNP MAS NMR was taken as an indication for a local electric field, leading to a hypothesis about the origin of the remarkable strength of the redox potential of the primary electron donor P680 (Matysik et al., 2000a; Diller et al., 2005).

The illumination setup that has been used for the photo-CIDNP experiment is designed for a standard Bruker wide bore MAS NMR probe as shown in Figure 1.3. The setup consists of a xenon arc lamp equipped with collimation optics, a liquid filter and glass filters, a focusing

element and a light fibre. The light is transported from the xenon arc lamp to the stator inside the probe with the light fibre (Matysik et al., 2000b).

A standard continuous illumination experiment can be performed with a Hahn echo pulse sequence for the 1D data sets or a modified Radio-Frequency Driven Recoupling sequence (RFDR) or spin diffusion experiments, with the cross polarization (CP) step replaced by a ^{13}C $\pi/2$ pulse, for the 2D dipolar correlation spectra.

1.2.3 Mechanism of photo-CIDNP in solids

Photo-CIDNP in solution NMR is explained by the radical-pair mechanism (RPM). The RPM relies on the different chemical fate of diffusing nuclear-spin selected reaction products (Closs and Closs, 1969; Kaptein and Oosterhoff, 1969; Hore and Broadhurst, 1993; Goez, 1997). However, RPM is not feasible in the solid-state or for cyclic reactions.

Initially, the net nuclear polarization providing photo-CIDNP in solids was assumed to be due to the significant differential relaxation (DR) between the nuclear spins in the special pair triplet ^3P and the nuclear spins in the singlet ground state of P, which would break the symmetry between the two branches (McDermott et al., 1998). However, it has been demonstrated experimentally, that the DR mechanism is not important for RCs from *Rb. sphaeroides* WT (Matysik et al., 2001a; Matysik et al., 2001b; Schulten et al., 2002). Subsequently, two mechanisms have been proposed. First, the electron-electron-nuclear three-spin mixing (TSM) mechanism, in which net nuclear polarization is created in the spin-correlated radical pair due to the presence of both anisotropic hyperfine interaction and coupling between the two electron spins (Jeschke, 1997, 1998). Second, the Differential Decay (DD) mechanism, in which a net photo-CIDNP effect is caused by anisotropic hyperfine coupling without an explicit requirement for electron-electron coupling if spin-correlated radical pairs have different lifetimes in their singlet and triplet states (Polenova and McDermott, 1999). As the two contributions may have different sign, control over both mechanisms may provide a tool to drive intensities in MAS NMR experiments far beyond the Boltzmann state (Jeschke and Matysik, 2003).

The interpretation of the photo-CIDNP intensities and their quantification requires a thorough understanding of the mechanisms that cause the build of this non-equilibrium polarization. Part of the present work aims at resolving the precise mechanisms behind the photo-CIDNP in different biological species. The information may lead to the extension of the solid-state photo-CIDNP approach to other systems.

1.3 Scope of this thesis

This thesis provides a novel experimental method for studying the electronic ground state of the photochemically active cofactors at atomic resolution. Enhancement in NMR intensities achieved with photo-CIDNP raises expectation for a new method that can overcome the

intrinsic insensitivity and non-selectivity of MAS NMR. **Chapter 2** deals with the magnetic-field dependence of photo-CIDNP in *Rb. sphaeroides* WT. The observed field dependence agrees with simulations that assume two competing mechanisms of polarisation transfer from electrons to nuclei, the three-spin mixing (TSM) and the differential decay (DD). The data reveal a ratio of the electron spin density on the special pair cofactors of 3:2 in favour of the P_L in the radical cation state. In **Chapter 3,** the field dependence of photo-CIDNP in *Rb. sphaeroides* R26 is investigated and the observed difference in the photo-CIDNP spectrum between the *Rb. sphaeroides* WT and its mutant R26 is explained. In **Chapter 4,** RCs from *Rb. sphaeroides* WT with site-directed ^{13}C labeled BChl and BPhe are investigated with photo-CIDNP MAS NMR dipolar correlation spectroscopy. The strong enhancement in NMR intensities, at a low field strength of 4.7 T enables, via 2D photo-CIDNP experiments, the assignment of signals of the special pair, the accessory BChl and the BPhe in the RCs. In **Chapter 5,** studies on the photosynthetic units are presented, suggesting for the first time anisotropy effects of photo-CIDNP. In **Chapter 6,** a brief overview of the mechanisms involved in photo-CIDNP is presented. A few ideas for future applications of photo-CIDNP are also introduced.